

The XMM/RGS Effective Area

C.P. de Vries ¹, A.J.F. den Boggende ¹, G. Branduardi-Raymont, ³, H. Brauning ⁵, A.C. Brinkman ¹, J. Cottam ², J.W. den Herder ¹, S.M. Kahn ², F.B.S. Paerels ¹, A. Rasmussen ², J. Spodek ², C. Erd ⁴

ABSTRACT

The effective area of the XMM Reflection Grating Spectrometer (RGS) has been measured at the MPE X-ray long beam facility (Panter). This report describes the analysis methods used. The results are compared with the theoretically expected effective area.

1. Introduction

Two of the three X - ray telescopes onboard XMM are fitted with the Reflection Grating Spectrometer(RGS) instrument. This instrument is capable of providing high resolution X - ray spectra in the range of 5 - 35 Å. For these telescopes, part of the X-rays, after being focused by the mirrors are deflected by a set of 182 reflection gratings. The spectral orders (mainly order -1, -2 and -3) are projected onto a set of backside illuminated CCD's in the RGS camera (RFC). These CCD's closely follow the Rowland circle. For performance monitoring and calibration purposes a set of calibration sources is mounted close to the CCD bench. CCD's are read-out sequentially in frame transfer mode and are operated at low temperature to reduce dark current. CCD integration times are sufficiently short to allow single photon detection. Combined with the intrinsic energy resolution of the CCD's the various spectral orders, which overlap spatially on the camera, can be very well separated. Hence, no confusion between spectral orders exist.

2. Effective area measurements at Panter

The RGS effective area was measured at the MPE long beam X-ray facility (Panter). Mirror, grating box and camera were mounted on moveable tables, such that positions and angles of these

¹SRON, Space Research Organisation of the Netherlands, Sorbonnelaan 2, 3584 CA UTRECHT, Netherlands

²Columbia University, 538 West 120th. Street, NY 10027 NEW YORK, U.S.A

³MSSL, Mullard Space Science Laboratory, Holmbury St. Mary, RH5 6NT Dorking, SURREY, U.K.

⁴ESA, Keplerlaan 1, 2200 AG, NOORDWIJK, Netherlands

⁵MPE, Panter X-ray Test Facility, Gautinger-Strasse 45, D-82061 Neuried, Germany

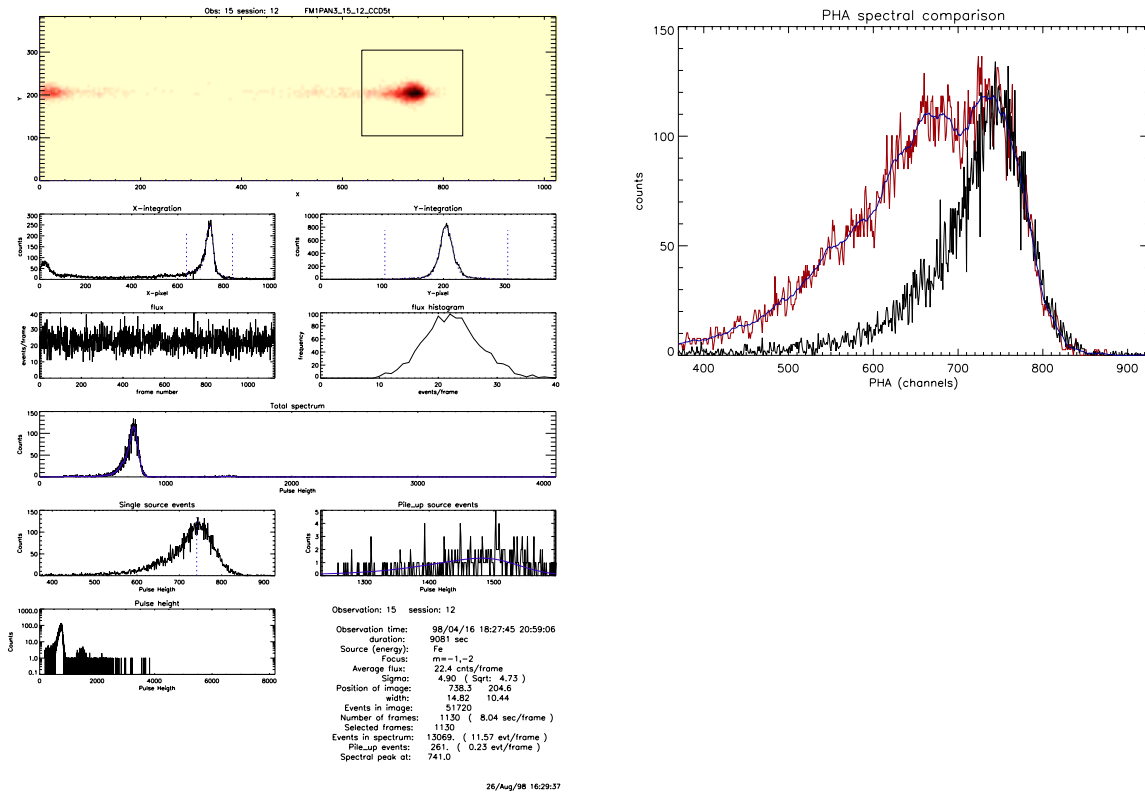


Fig. 1.— Sample measurement (Fe-L line) The left half shows a sample of the standard analysis, plotting the $m=-1$ CCD image (top) displaying the main Fe-L line inside the solid box. On the extreme left of the image there is a second satellite line, also clearly seen in the x-crosscut below the image. On the right half the CCD pulse spectrum is shown for the $m=0$ (broad, two component shape) and the $m=-1$ (narrow single component peak). The $m=0$ includes both the main Fe-L and its satellite. The comparison of the pulse shapes allows to estimate which fraction of the incident beam corresponds to the main Fe-L line. In addition the left half standard analysis shows the fitting procedure for pile-up events. These are multiple photons hitting the same CCD pixel twice within a single integration time. To obtain an estimate of these, the main CCD pulse (single source events) is auto-convolved. This convolved function is fitted to the CCD pulse spectrum at higher pulse-heights (pile-up source events). The scale factor determines the number of pile-up events.

items could be changed with respect to each other. At the opposite end of the vacuum tube, about 120m distance, an X-ray target source with a variety of different targets was available. Targets giving cleanest, preferably single or well separated X-ray lines were selected. Targets used were (in increasing energy): O,Fe,Cu,Mg,Al and Si.

X-ray line flux in *counts/cm²/sec* in the incident beam was measured by the RGS camera itself, when the grating box and mirror were moved out of the beam. Knowing the Quantum-Efficiency (QE) of the CCD, the CCD surface area and the spectral characteristics, the flux can be calculated. Taking the ratio of the counts measured by the complete RGS (using the same RGS camera) in the various spectral orders of the X-ray line and the X-ray beam flux gives the effective area of the instrument. The incident beam flux was measured both before and after the spectral measurement, to check on target source stability.

Many target source spectra show contaminating lines and/or continuum close to the main X-ray lines used to measure the effective area. In the beam-flux measurement the CCD does not resolve the X-ray line of interest, while the complete RGS instrument does. To estimate the fraction of flux in the X-ray line, the CCD pulse spectra of the m=0 order were compared with the m=-1 CCD pulse spectra. The uncertainties in this estimate are the main systematic error in the effective area measurement. Fig 1 shows a sample of this comparison for a (badly contaminated) spectrum.

3. Theoretically expected effective area

The RGS effective area can be thought of as the combination of a number of factors:

- Mirror effective area. This has been measured by MPE at Panter. Since at Panter the source is at finite distance, internal vignetting within the mirror plays a role. For the flight situation, when sources are at infinite distance and there is no internal vignetting, the mirror effective area is expected to be a factor of 1.52 larger than measured at Panter.
- Grating efficiency. This can be theoretically calculated. (See contribution by J.Cottam et al.)
- Internal grating vignetting. For large grating exit angles (wavelength and order dependant) the reflected X-rays might hit the back side of the neighbouring grating, reducing effective area.
- CCD Quantum efficiency (QE). This can be theoretically calculated, based on materials thicknesses on the CCD. Theoretical computations are in reasonable agreement with actual measurements. Different CCD's have different layer thicknesses, meaning different QE's for different parts of the spectrum for different orders.

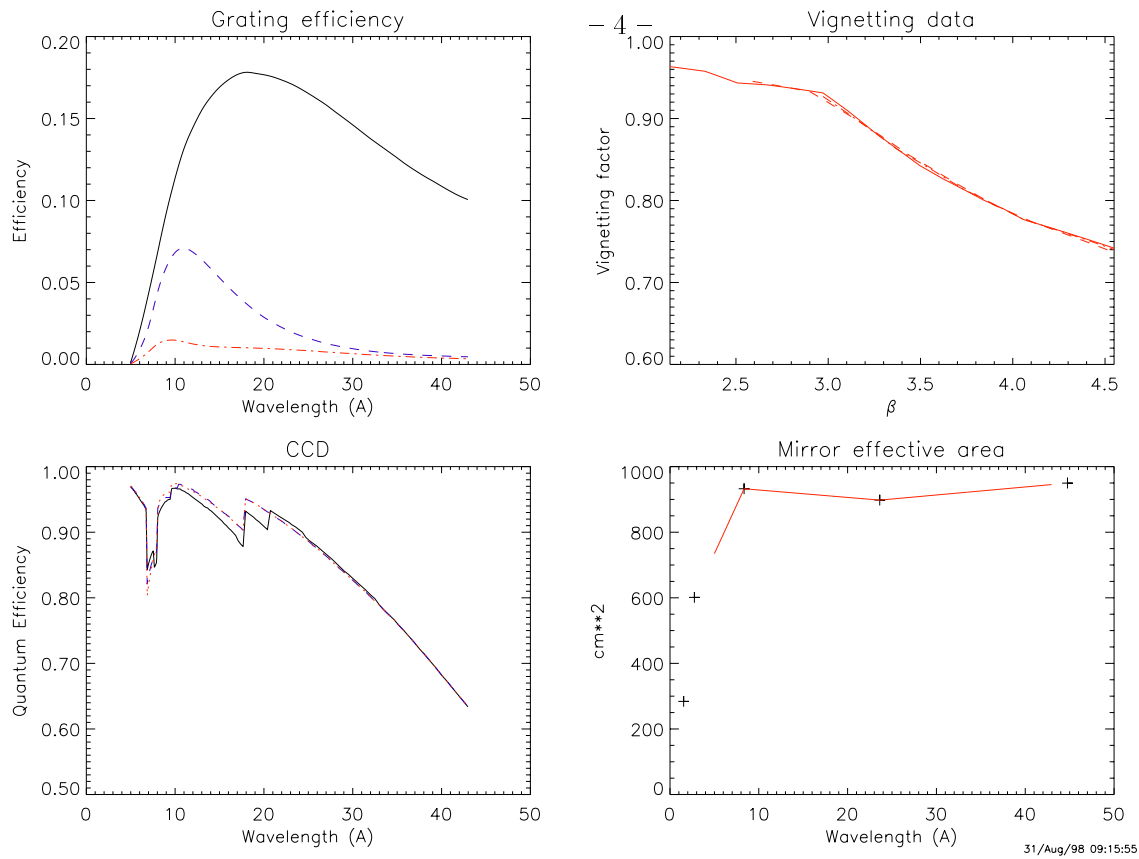


Fig. 2.— Effective area components:

- (top left) Theoretically computed single grating efficiency (see contribution by J.Cottam et al).
- (top right) Vignetting computed using a ray trace algorithm. It solely depends on grating exit angle β which can be related to wavelength and order via the dispersion equation $m\lambda = d(\cos(\beta) - \cos(\alpha))$ where m is the spectral order, λ the wavelength, d the grating groove distance and α the angle of incidence.
- (lower left) CCD Quantum efficiency based on absorption in the known CCD layers thicknesses. Different orders and wavelengths will hit different CCDs with each having a slightly different QE. Sharp features in the curves are caused by a combination of material absorption edges and changes in material layer thicknesses between different CCD's.
- (lower right) Mirror effective area as measured at Panter with source at finite distance. For infinite sources the mirror surface is expected to be larger by a factor of 1.52 .
- (not plotted) In addition there's a fixed factor of 0.37 which represents the fraction of the beam hitting a proper grating surface. The rest of the beam will either hit a support structure, or will go to the EPIC focus.

- Beam coverage. Part of the X-ray beam goes through the grating box without hitting a grating, to end up at the EPIC focus. Another part of the X-ray beam will hit the grating box support structure. Simulations show that only about 37% of the beam will hit a grating in the proper way, to form a spectrum.

Fig 2 gives an overview of the nature and magnitude of all these components.

4. Results

Fig 3 shows the final results. It compares both measurements and theoretical expectation. All results (data and theory) have been scaled to the expected flight situation, where internal mirror vignetting does not play a role. Both data and theory have their uncertainties. Theoretical grating efficiency overall uncertainty is about 5% but may be more uncertain at shorter wavelengths. Mirror effective area has been measured at few wavelengths only, while CCD-QE may be different due to e.g. CCD layer inhomogeneities. Overall agreement between theory and measurements is of order 10%, which is reasonable given the known uncertainties. Effective area for a single RGS around 15 - 20 Å in first order is about 70 cm^2 . It is expected that both RGS instruments will be the same in that respect.

5. Off-axis effective area

At Panter the relative off-axis response in the dispersion direction was measured by rotating the optical bench (mirror plus grating box). This was only done for one target source (Al). For these relative measurements, uncertainties about spectral characteristics of the source do not play a role. Main source of systematic errors in these measurements is the target source stability. Absolute off-axis effective area can be determined by scaling the on-axis observed number of counts to the known on-axis effective area for Al (see fig 3). The data are plotted in fig 4. Main component in the off-axis response is the mirror (4a). Deviations from the mirror response match the expected response for the total RGS quite well (4b). Apart from the mirror, other components in the relative off-axis response are the single grating response for other incidence angles, relative changes in internal grating vignetting and changes in the projected area of the gratings on the beam. The off-axis response is quite wavelength dependant, because the main component, apart from the mirror, is the grating efficiency. Since at Panter only one wavelength (Al) has been measured, the multi-wavelength response for in-flight off-axis sources has to rely on the grating theory (and possible in-flight measurements of known sources at different angles)

The cross-dispersion direction off-axis effective area accurately follows the mirror response.

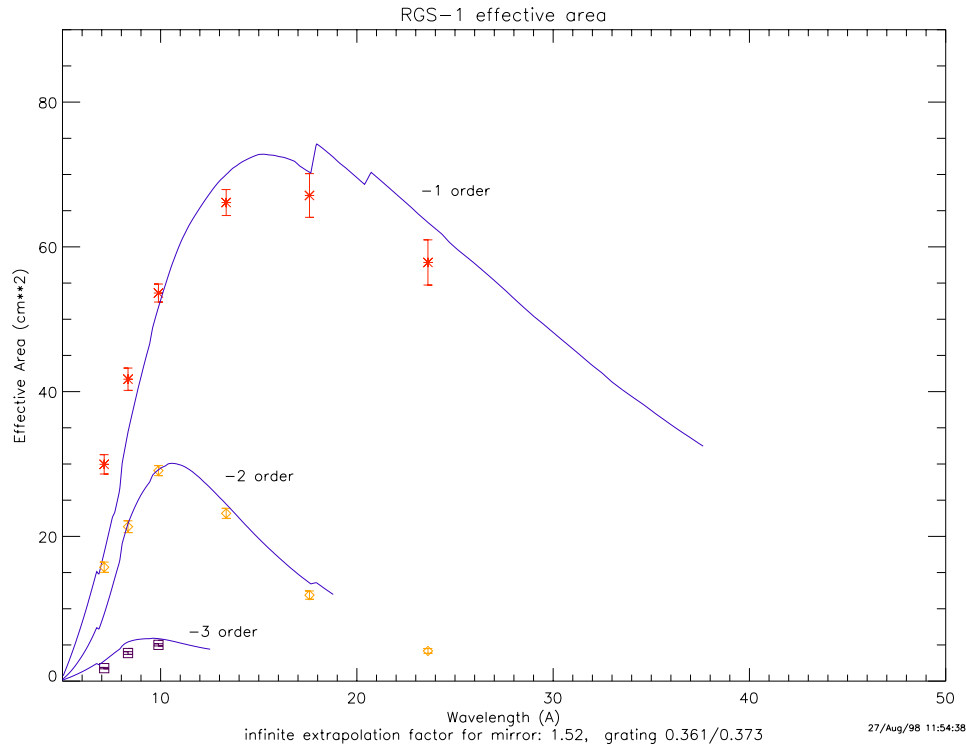


Fig. 3.— Expected theoretical effective area (curve) and measured data for the RGS, scaled to represent the inflight (infinite source distance) situation. The range of the solid curves reflect the true range in wavelengths for the different orders of the RGS for on-axis sources. The datapoint at 24 Å outside the range of the 2nd order was measured by moving the CCD camera to the proper position

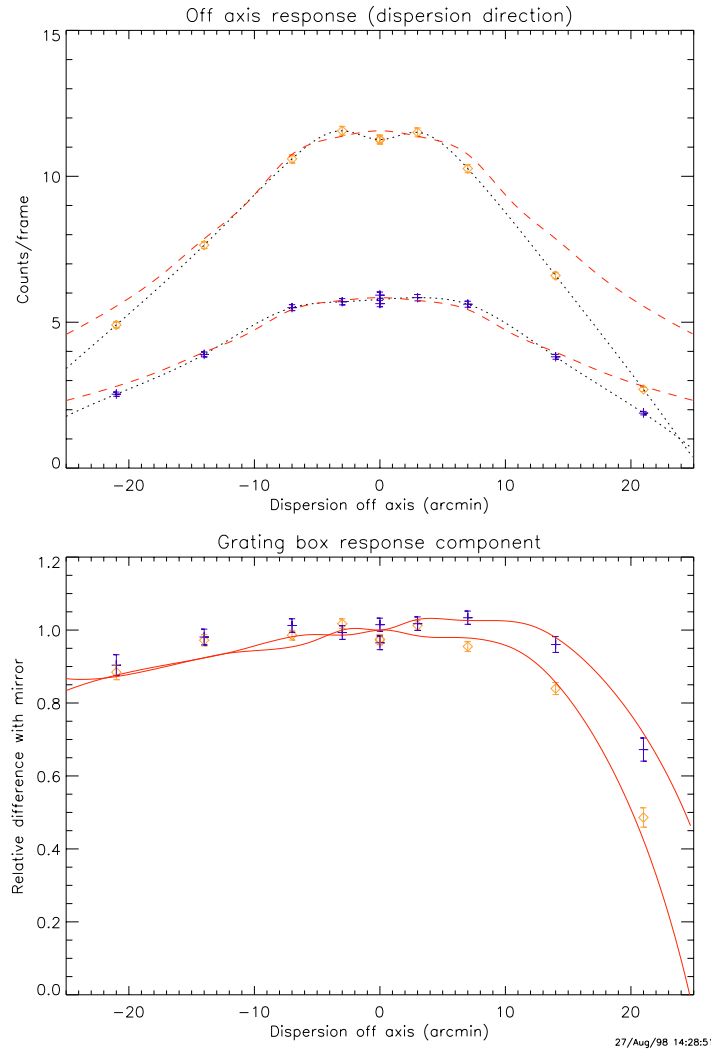


Fig. 4.— (top) Total relative off-axis response for the total RGS, which includes the mirror response. High line/points are first order, lower line/points are second order. Dashed line shows the mirror response only, while dotted line shows interpolation of data points. The error bars reflect the statistical errors. Additional systematic errors may be caused by the uncertainty of the X-ray target source stability. (bottom) Off-axis RGS response, but now the relative difference of the datapoints with respect to mirror response (see top figure) is plotted. Crosses are second order, diamond shape points first order. The solid line represents the theoretically expected response for the total box when measured single grating efficiency data are used. The single grating measurements are based on one grating only. It is known that differences of several percent may exist between gratings. Curves for the total box may therefore be slightly different.